A novel fuzzy logic control for a zero current switching-based buck converter to mitigate conducted electromagnetic interference

Zakaria M'barki, Kaoutar Senhaji Rhazi, Youssef Mejdoub
Laboratory of Networks, Computer Science, Telecommunication, Multimedia, CED Engineering Sciences,
Higher School of Technology, Hassan II University, Casablanca, Morocco

Article Info

ABSTRACT

This research provides a new control technique for mitigating conducted electromagnetic interference (EMI) in a buck converter designed for solar applications. Indeed, hard-switching direct current to direct current (DC-DC) converters, commonly used in industrial applications, pose a significant risk to the surrounding environment regarding electromagnetic compatibility (EMC). Usually, the fast-switching phase induces abrupt changes in current and voltage, which adds to substantial electromagnetic interference in both conducted and radiated modes and excessive auditory noise. An architecture based on the duality of soft-switching topology and fuzzy logic control technology is developed to address these issues. On the one hand, resonant circuit topologies are used to induce switches to achieve soft switching conditions, which subsequently lessen the effects of EMI. On the other hand, the adoption of fuzzy logic control technology is interesting since it can reduce electrical stresses during switching. Furthermore, the simulation results show that zero current switching (ZCS) soft-switching closed-loop fuzzy logic converters outperform typical open-loop converters and soft-switching closed-loop converters with proportional integral (PI) control in terms of EMC requirements.

Corresponding Author:

Zakaria M'barki
RITM Laboratory, Higher School of Technology, Hassan II University of Casablanca
Km 7 El Jadida Road-r.p.8, B.P. 20000, Casablanca-Morocco
Email: mbarki.ensem@gmail.com

1. INTRODUCTION

Improved power conversion systems, widely used in several industries such as choppers, and inverters, have become necessary for adapting to varied technologies and conditions. Advanced converter topologies were implemented to increase efficiency and electromagnetic interference (EMI) performance [1], increase frequency, and reduce footprint. Moreover, photovoltaic (PV) modules to convert sunlight directly into power have grown convenient in recent years. DC to DC conversion technology is widely used in power electronics, engineering, and drives to support a broad range of specific loads. We decided to use the buck conversion system to reduce the output voltage of our load for this research application. We take a quasi-DC voltage at the solar panel's output for simplicity.

The buck converter is undoubtedly one of the most significant generators of electromagnetic interference in the environment [2]. It is distinguished by its circuit's simplicity and its control method's robustness. Its conventional control is based on pulse width modulation (PWM) hard switching [3]. This structure introduces fast switching constraints owing to voltage and current gradients ($\frac{dv}{dt}$ and $\frac{di}{dt}$), which favor

disruptive emissions, while also contributing to additional losses in power semiconductor switching devices due to the increased switching frequency. In this context, substantial research has already been conducted to overcome its expected flaws, resulting in switches with a soft-switching structure [4]. The benefit of this type of switching is that devices are only switched when the switch's voltage and current are both zero, resulting in zero voltage switching (ZVS) or zero current switching (ZCS) [5], [6]. In recent years, ZCS has become increasingly relevant in power converters. One of the most popular advanced ZCS schemes is the zero current switching quasi-resonant buck converter (ZCS-QRC) [7]. Resonant circuits consisting of inductance and capacitance (LC) are incorporated into standard converter topologies to limit the current gradient when the main switch is closed. This ensures that conducted electromagnetic disturbances are reduced, contributing to good electromagnetic compatibility (EMC) gain.

In the same vein, new control approaches have been implemented in recent years to add intelligence to classic control systems. Furthermore, many investigations have been performed on controller design based on classical and modern control theory. Various controllers, such as the commonly used classic proportional integral derivative (PID) controllers, can be found in the literature [8]. They're well-suited to precise linear mathematical models, which is not usually the case in industrial systems. Then there are fuzzy logic controllers (FLC) [9], which are incredibly effective at dealing with mathematically ill-defined or imprecise systems, particularly those with non-linearity. They're also resistant to input signal variations and load fluctuations. Fuzzy control is now one of the most extensively used approaches for controlling DC-DC converters [10], and it is increasingly being integrated into numerous industrial applications. The control of our researched technology, the buck converter, will be based on this technique. Its main advantage is its capacity to effectively lower EMI levels and contribute to EMC compliance [11]. Therefore, the originality of this study is, of course, the use of a dual approach that combines the EMC strengths of the two previously anticipated ways. Compared to the other methodologies, an investigation of the spectrum content associated with electromagnetic interferences produced positive findings.

In this article, a buck converter is modeled, and an EMI measuring technique is used. Early comparisons show that this hard-switching converter releases significantly more conducted emissions than soft-switching converters. The fuzzy logic controlled soft-switching buck converter is explained first, followed by a comparison of conducted EMI with open-loop and proportional-integral (PI) regulated circuits. Finally, a brief conclusion is offered.

2. BUCK CONVERTER STUDY AND MEASUREMENT OF CONDUCTED DISTURBANCES

The buck converter is a typical DC-DC converter that efficiently converts high- and low-voltage. It has a wide range of applications [12]. The investigated converter comprises an IRFP450 type metal-oxide-semiconductor field-effect transistor (MOSFET) and a BYT12P-600 reference diode and operates in a continuous conduction mode. Figure 1 depicts the global diagram of the investigated system as implemented in the MATLAB/Simulink environment. Figure 1 shows a simplified internal design of an open-loop buck converter. The MOSFET is turned on and off by a PWM control signal with a duty cycle of D that represents the percentage of time the MOSFET is on. The DC transfer function is an equation that connects the input voltage, the output voltage, and the duty cycle D so that:

$$V_{out} = V_{in} * \text{D}. \tag{1}$$

A low-pass filter consists of an inductor and a capacitor. This low-pass filter smooths the MOSFET's switching activity and generates a stable DC voltage. It is utilized to keep the inductor's maximum current ripple (ΔI_L =20%) and the load's maximum voltage ripple (ΔV_O =2%) to a minimum as shown in Figure 2. The calculation of the components of this filter is given by (2).

$$L_F = \frac{(V_{in} - V_O)\ \mu\ T_s}{\Delta I_L};\ \ C_F = \frac{\Delta I_L\ T_s}{8\,.\,\Delta V_O} \tag{2}$$

This buck converter is designed to meet the following requirements, as indicated in the Table 1.

Electromagnetic noise that can develop harmonics and propagate via electromagnetic conduction or radiation, affecting a wide frequency range, is known as electromagnetic interference [13]. As a result, these disturbances can damage or even disrupt the operation of nearby electrical circuits. Conducted and radiated EMI are the two types of EMI [14]. Electromagnetic energy created by an electronic device can be transmitted or linked through metallic conductors, resulting in conductive emissions [15], [16]. Radiated emissions [17], on the other hand, are electromagnetic radiation generated by electronic equipment propagated in free space. Figure 3 depict the many types of EMI.
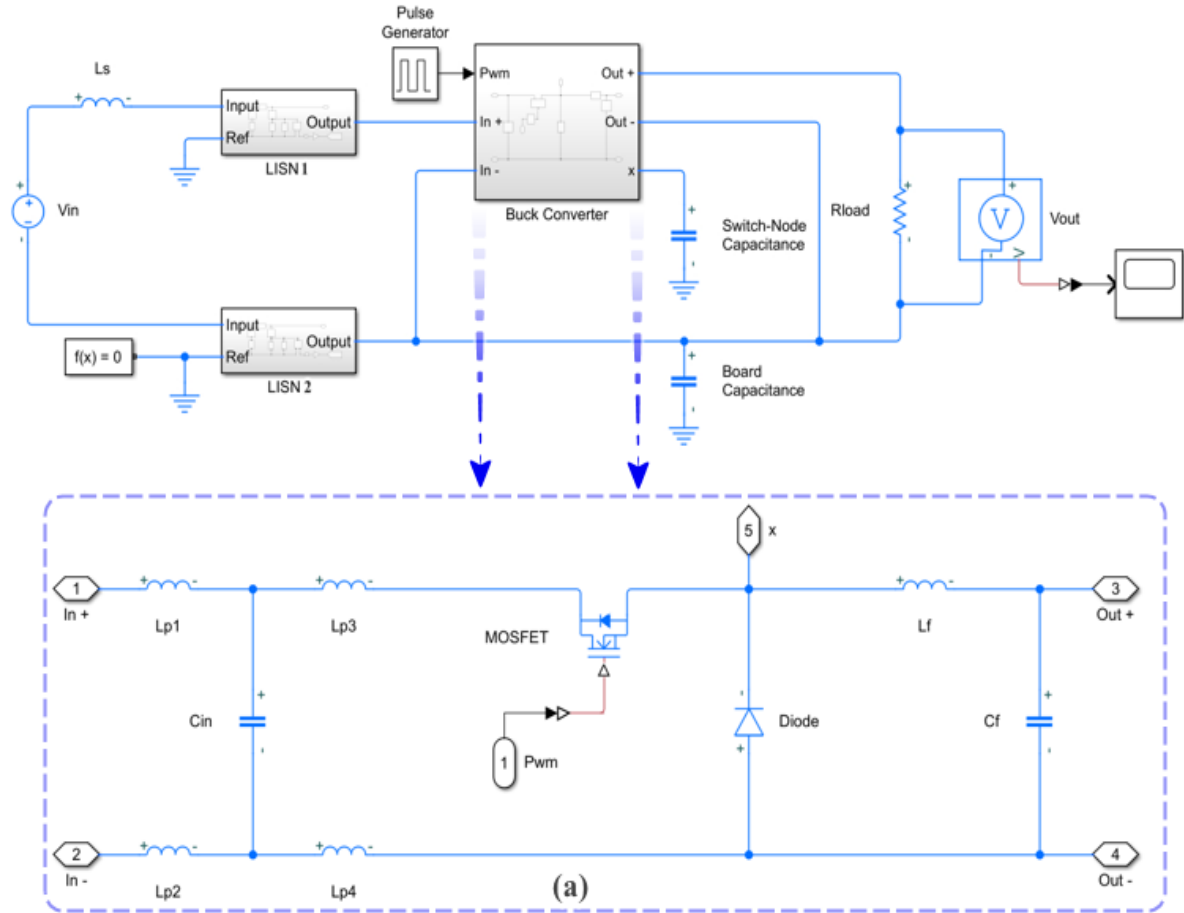
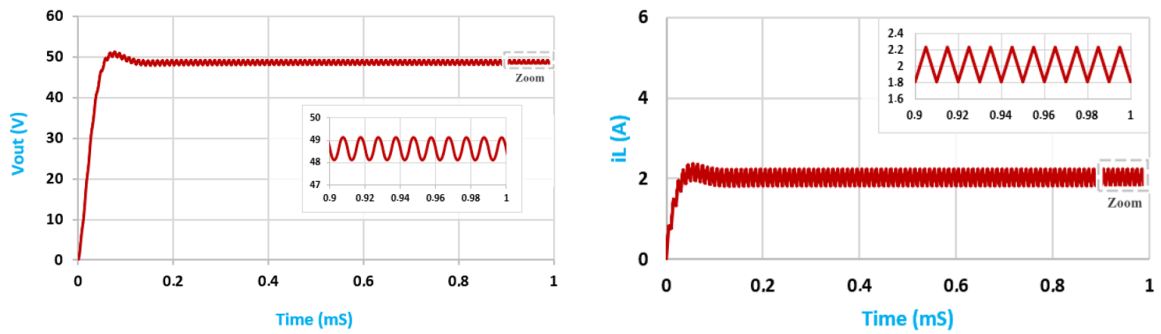Figure 1. The entire system architecture with the internal layout of the buck converter's block

Figure 2. The buck converter's steady-state waveforms (i_L and V_{out})

Table 1. Simulation parameters

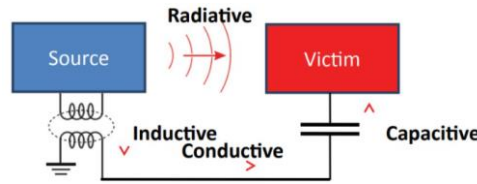| Parameter	Value
Input voltage V_{in}	100 V
Output voltage V_O	50 V
Load resistance R_L	24 Ω
Switching frequency $f_s = \frac{1}{T_s}$	100 KHz
Inductance L_F	600 µH
Capacitance C_F	520 nH
Conversion ratio M=$\frac{V_O}{V_{in}}$	50%

Figure 3. EMI's several kinds

In this section, only conducted EMI will be quantified [18]. A measurement tool has been created for this purpose. A line impedance stabilization network, or "LISN", is an EMC-required device as shown in Figure 4(a). It is a gadget that detects conducted EMI and works similarly to a filter installed between the equipment under test and the power supply network. Its principal purpose is to separate the equipment under test from the network, which may contain common-mode and differential-mode disturbances as shown in Figure 4(b). The following relations indicate disturbances related to the common mode (V_{mc}) and differential mode (V_{md}).

$$V_{MC} = \frac{V_1 + V_2}{2} \; ; V_{MD} = \frac{V_1 - V_2}{2} \tag{3}$$
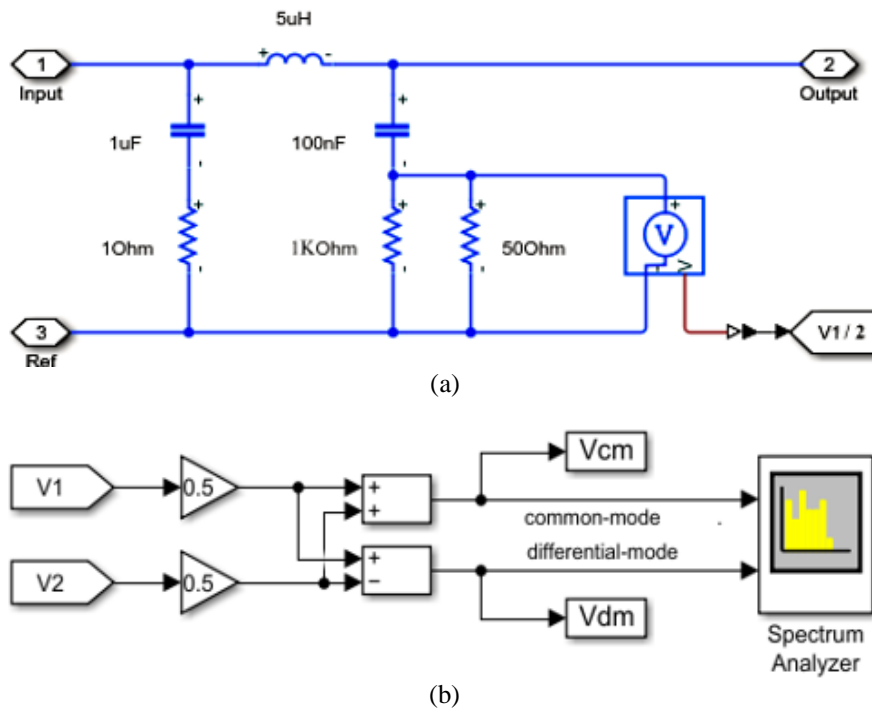

(a)

(b)

Figure 4. Conducted EMI measurements using (a) the line impedance stabilization network (LISN) tool with its internal schematic for and (b) quantifying disturbances in differential and common mode

3. PROPOSED METHOD
3.1. Soft switching: zero current switching (ZCS)

In Most traditional power electronic systems produce conducted emissions that propagate at frequencies between 150 kHz and 30 MHz. The electrical strains imposed by semiconductor-based switches during commutation, known as hard switching, induce fast fluctuations in current and voltage ($\frac{di}{dt}$ and $\frac{dv}{dt}$), imposing strict electromagnetic compatibility requirements. New soft-switching power electronics topologies are currently being developed to address these previously predicted drawbacks [19]. The use of a resonant circuit around the semiconductor switches that includes extra elements (inductor, capacitor, or diode) reduces switching losses by creating ZVS settings or ZCS conditions.

A resonant inductor in series with the primary switch is frequently employed in ZCS converters to resonate the current across the switch to zero on opening and restrict the $\frac{di}{dt}$ on closure. In ZVS converters, a resonant capacitor is employed in parallel with the primary switch to restrict the $\frac{dv}{dt}$ on opening and to resonate the voltage across the switch to zero on closing. The ZCS approach and its efficiency in reducing EMI emissions will be the subject of this research [20]. The following characteristics describe the design of quasi-resonant buck converters running at zero current:

− Normalized resonance frequency: $f_n = \frac{f_s}{f_r}$ with $f_r = \frac{1}{2\,\pi\sqrt{L_r\,C_r}}$

− Normalized characteristic impedance: $Z_n = \sqrt{\frac{L_r}{C_r}}$

− Normalized load resistance: $Q = \frac{R_{load}}{Z_n}$

− Conversion ratio: $M = \frac{V_{out}}{V_{in}}$

The schematic of the modeled buck converter is shown in Figure 5(a). This schematic is subdivided into five modes of operation as shown in Figure 5(b), depending on the state of the main switch and the freewheeling diode. The output current and voltage are then supposed to be continuous by assuming that the output filter's inductance and even capacitance are significantly larger than the resonance's inductance and capacitance.
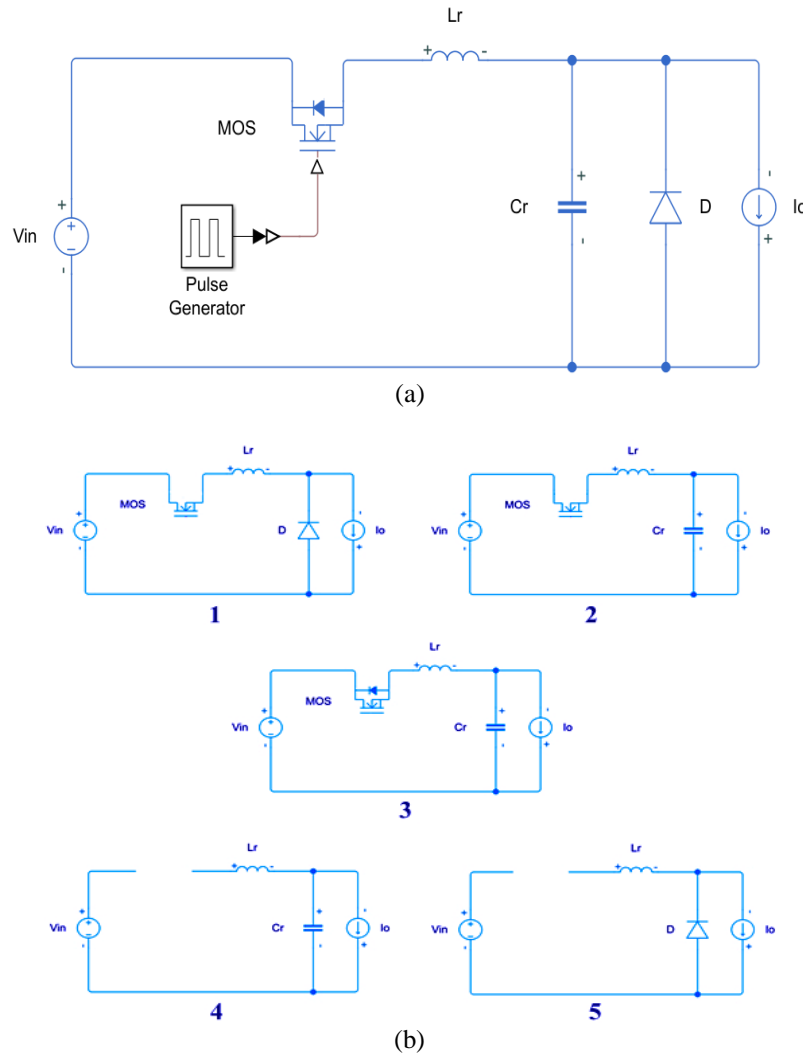

(a)

(b)

Figure 5. Buck quasi-resonant converter with (a) zero current switching scheme and its (b) equivalent circuits operating modes

3.1.1. Mode 1

At the start of this mode, the MOSFET switch is turned on. Following that, we can see that the current of the resonant inductor I_{Lr} increases linearly while the diode's current I_D declines until it reaches zero. Therefore, the switch's ZCS activation is assured. The subcircuit at this interval is depicted in Figure 5(b) 1. As a result, we have (4):

$$I_{Lr} = \frac{V_{in}}{L_R} \, t; \, V_{Cr} = 0 \tag{4}$$

when the resonant inductor's current hits I_0, the diode switches off, and this mode ends. This mode's duration is expressed by: $\tau_1 = t_1 = \frac{I_0 * L_r}{V_{in}}$.

3.1.2. Mode 2

As indicated in Figure 5(b) 2, this mode begins when diode D is open-circuited. A resonant stage is made up of the inductor L_r and capacitor C_r. As a result, the inductor current I_{Lr} and the resonant capacitor voltage continue to grow sinusoidally. The associated equations of state can be established as (5).

$$I_{Lr} = I_0 + \frac{V_{in}}{Z_n} \sin w_r \, (t-t_1); \, V_{Cr} = V_{in}(1-\cos w_r \, (t-t_1)); \, I_0 \leq \frac{V_{in}}{Z_n} \tag{5}$$

This interval will expire when the inductor current reaches zero. This mode's duration is calculated as: $\tau_2 = t_2 - t_1 = \frac{1}{W_r}[2\pi - \alpha]$ avec $\alpha = sin^{-1}(\frac{Z_n I_0}{V_{in}})$.

3.1.3. Mode 3

Resonant current passes through the switch body diode at the start of this interval, as represented by the subcircuit in Figure 5(b) 3. The resonant elements start to oscillate negatively. This is the ZCS interval during which switch deactivation is guaranteed. For the resonant elements, the state equations are the same as before.

3.1.4. Mode 4

Figure 5(b) 4 presents the subcircuit for this interval. The resonant capacitor discharges linearly with an $\frac{I_0}{C_r}$ slope at the start of this mode. Because the voltage is negative, the diode remains off. Below are the state equations for the resonant elements.

$$I_{Lr} = 0; \, V_{Cr} = \frac{-I_0}{C_r}(t - t_2) + V_{in} \, (1-\cos \alpha) \tag{6}$$

This mode's duration is determined by: $\tau_3 = t_3 - t_2 = \frac{V_{in} C_r}{I_0}(1-\cos \alpha)$. The capacitor voltage decreases to zero and the output diode turned on, signaling the end of this interval.

3.1.5. Mode 5

The main switch remains off in this mode, which is the shutdown state of any typical converter, but the diode begins to conduct. Figure 5(b) 5 depicts the relevant subcircuit. The output current begins the freewheeling phase through the diode as soon as the switch is turned off, and this mode continues as long as the switch is turned off. The resonant elements' state equations are listed.

$$I_{Lr} = 0; \, V_{Cr} = 0 \tag{7}$$

This mode will stop at $t_4 = T_s$, and will last for: $\tau_4 = T_s - \tau_3 - \tau_2 - \tau_1$. Figure 6 illustrates the theoretical waveforms of the resonant tank. We can express the voltage gain using the concept of energy conservation as:

$$M = \frac{f_n}{2\pi}(\frac{M}{2Q} + 2\pi - sin^{-1}(\frac{M}{Q}) + \frac{Q}{M}(1 - \sqrt{1 - (\frac{M}{Q})^2})) \tag{8}$$

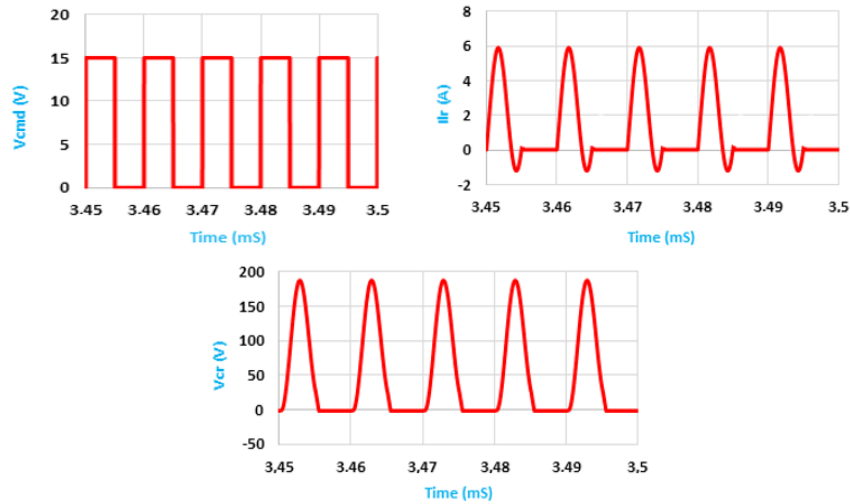$$D = \frac{f_n}{2\pi}(\frac{M}{Q} + 2\pi - sin^{-1}(\frac{M}{Q})) \tag{9}$$

Figure 6. Voltage and current for the ZCS method

For various loads Q, the conversion rate M is plotted against the normalized frequency as shown in Figure 7. Numerical analysis using the Newton-Raphson method was used. The output voltage in the ZCS topology is shown to be linearly proportional to the control frequency.
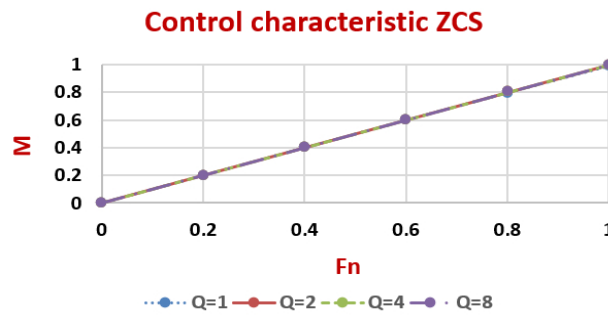

Figure 7. The conversion ratio characteristic based on the normalized load

Based on the preceding paragraph's assessment of the Quasi-Resonant buck converter, the following findings may be given, assuming that M=0.5 and Q=1:

− The conversion ratio is thus expressed as: $M = \frac{f_n}{2\pi}(\frac{1}{4}+2\pi-\frac{\pi}{6}+2(1-\frac{\sqrt{3}}{2}))\approx f_n$.

− The resonant frequency: $f_r = \frac{f_s}{M}$

− The duty cycle: $D = \frac{f_n}{2\pi}(0.5 +2\pi-\frac{\pi}{6})\approx f_n$.

The resonant inductor and capacitor are calculated by these formulas:

$$L_R = \frac{Z_n}{2\pi f_r} \; ; C_R = \frac{1}{2\pi \, f_r \, Z_n} \qquad (10)$$

The Table 2 summarizes the preceding discussion.

Table 2. The buck ZCS-QRC converter parameters

Component	Normalized value
Inductance L_R	20 μH
Capacitance C_R	35 nH
Resonant frequency f_r	200 KHz
Duty cycle D	~50%

3.2. Control of the buck converter with fuzzy logic and a PI controller
3.2.1. Fuzzy logic controller design

Fuzzy control has been widely used in industrial processes in recent years. It is based on a heuristic model, which consists of a set of rules based on human experience rather than mathematical equations. A fuzzy controller frequently follows a process that consists of three steps as shown in Figure 8:
− Input fuzzification: converts input values into fuzzy quantities.
− Inference (with rule base): applies the rules to the fuzzified inputs to make decisions.
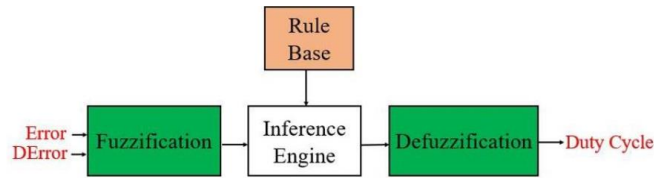− Defuzzification: the process of converting fuzzy decisions into numerical output values.

Figure 8. The fuzzy logic controller diagram

This paper uses a fuzzy logic controller to regulate a buck DC-DC converter [21]. The MATLAB/Simulink software was used to simulate this controller as shown in Figure 9. Indeed, the controller applies these rules and gives the different duty cycles that are sent to the buck converter switch through a PWM generator based on the input values obtained, namely the difference between the output voltage V_{out} and the desired voltage V_{ref}, called error (E), as well as the error variation (dE).
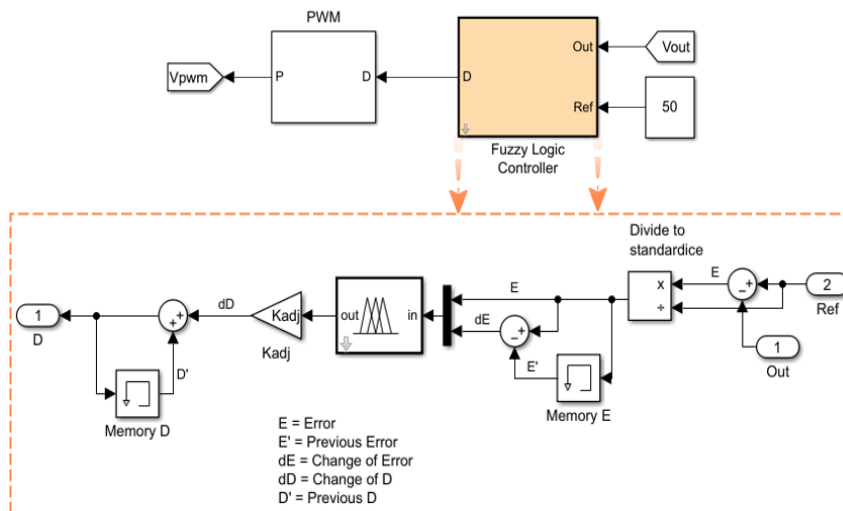

Figure 9. FLC for DC-DC buck converter

The fuzzy logic algorithm's rules are often "if and then" statements. In this situation, "if" refers to the condition, and "then" refers to the result. When the converter's load voltage is lower than V_{ref}, for example, the duty cycle must be increased and aimed at that voltage. Fuzzy logic is a type of mathematical logic based on the concept of "degree of truth", in which it distinguishes between true and false states. Five linguistic variables were employed to quantify the error (E) and the change of error (dE) when building the controller based on Mamdani's fuzzy inference technique: negatively large (NL); negatively small (NS); zero (Z); positively small (PS); and positively large (PL). Membership functions such as triangular and trapezoidal functions are utilized to minimize computations. Figure 10 depicts the membership functions dedicated to the error (E) shown in Figure 10(a) and the variation (dE) of the error shown in Figure 10(b), as well as the output D shown in Figure 10(c). However, the fuzzy inputs/outputs rules are arranged in Table 3. The resulting control surface of the proposed fuzzy controller is illustrated in Figure 11.
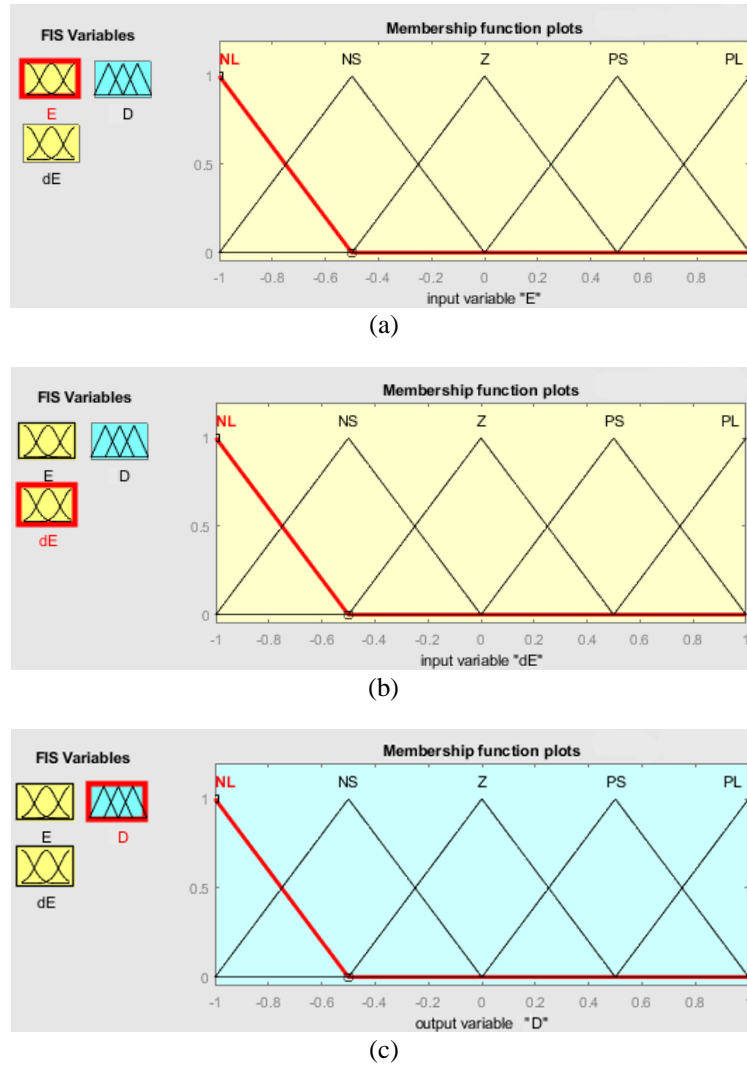
(a)

(b)

(c)

Figure 10. Membership function for (a) input error, (b) change in error, and (c) output variable

Table 3. Rule base for fuzzy controller

E / dE	NL	NS	Z	PS	PL
NL	NL	NL	NL	NS	Z
NS	NL	NL	NS	Z	PS
Z	NL	NS	Z	PS	PL
PS	NS	Z	PS	PL	PL
PL	Z	PS	PL	PL	PL
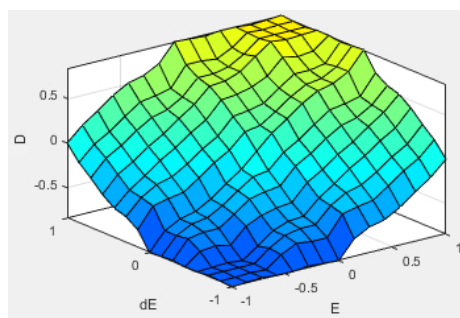
Figure 11. The control surface of the fuzzy controller

3.2.2. Proportional integral control system

Furthermore, the performance of a traditional PI controller is compared to that of a fuzzy controller. The main focus will be on the efficiency of these control approaches, as measured by the decrease in voltage and current limitations created during the switching process [22]. The PI controller is automatically tuned using the Simulink tool's "PID tuning" interface to achieve an ideal system design and match the specifications' stability, speed, and accuracy requirements. A proportional gain (K_p) that reduces the rise time and an integral gain (K_i) that eliminates the error in steady state are the parameters of a PI controller. The parameters are listed in the Table 4.

Figure 12 describes the variation of the buck-ZCS converter's output voltage V_{out} in the open loop illustrated in Figure 12(a) and closed loop of the PI controller and the fuzzy controller shown respectively in Figures 12(b) and 12(c). Compared to conventional approaches, it becomes evident that the fuzzy logic controller allows for more robust control [23]. Indeed, this controller has the shortest settling time of 0.15 milliseconds and the slightest output voltage ripple. On the other hand, the PI controller has an exact output voltage but ripples and overshoots, as well as a much longer settling time.

Table 4. Tuned PI values

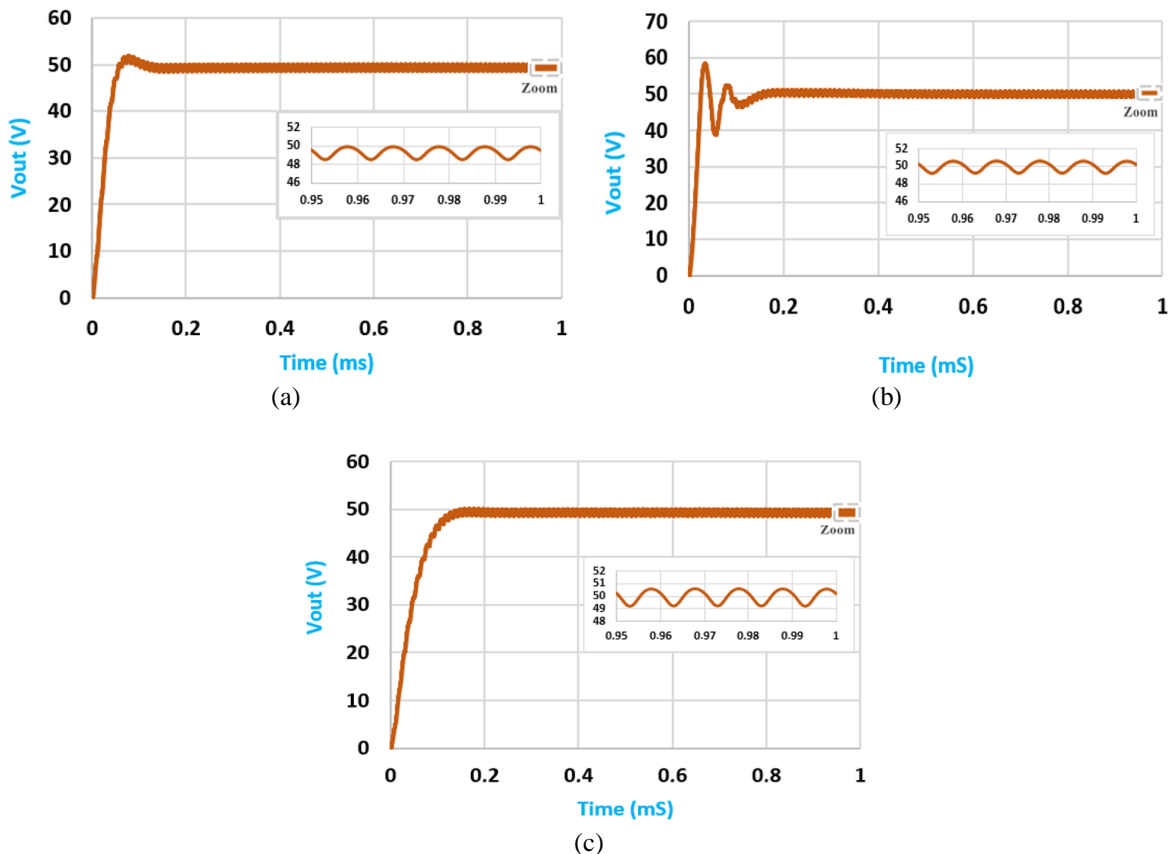| Parameters	Values
K_p	0.05
K_i	400

(a)

(b)

(c)

Figure 12. The plot of output voltage V out under ZCS control conditions in (a) open loop, (b) closed loop by PI controller, and (c) closed loop using the fuzzy logic controller

4. SIMULATION RESULTS AND DISCUSSION

The measurement of electromagnetic disturbances based on conduction is of particular importance in this section. Even so, this investigation aims to evaluate how a MOSFET-based step-down chopper affects the EMC of a DC voltage source. This research was carried out in a MATLAB/Simulink environment. The

LISN circuit depicted in Figure 4(a) is commonly used to measure the conducted EMI produced in the buck converter. The outputs of the common noise voltage V_{cm} and the differential noise voltage V_{dm} are evaluated. As illustrated in Figure 13, we are now interested in analyzing these disturbances' spectral content for the proposed approaches: DPWM method shown in Figure 13(a), ZCS method shown in Figure 13(b), ZCS-PI method shown in Figure 13(c) and ZCS-FLC method shown in Figure 13(d).

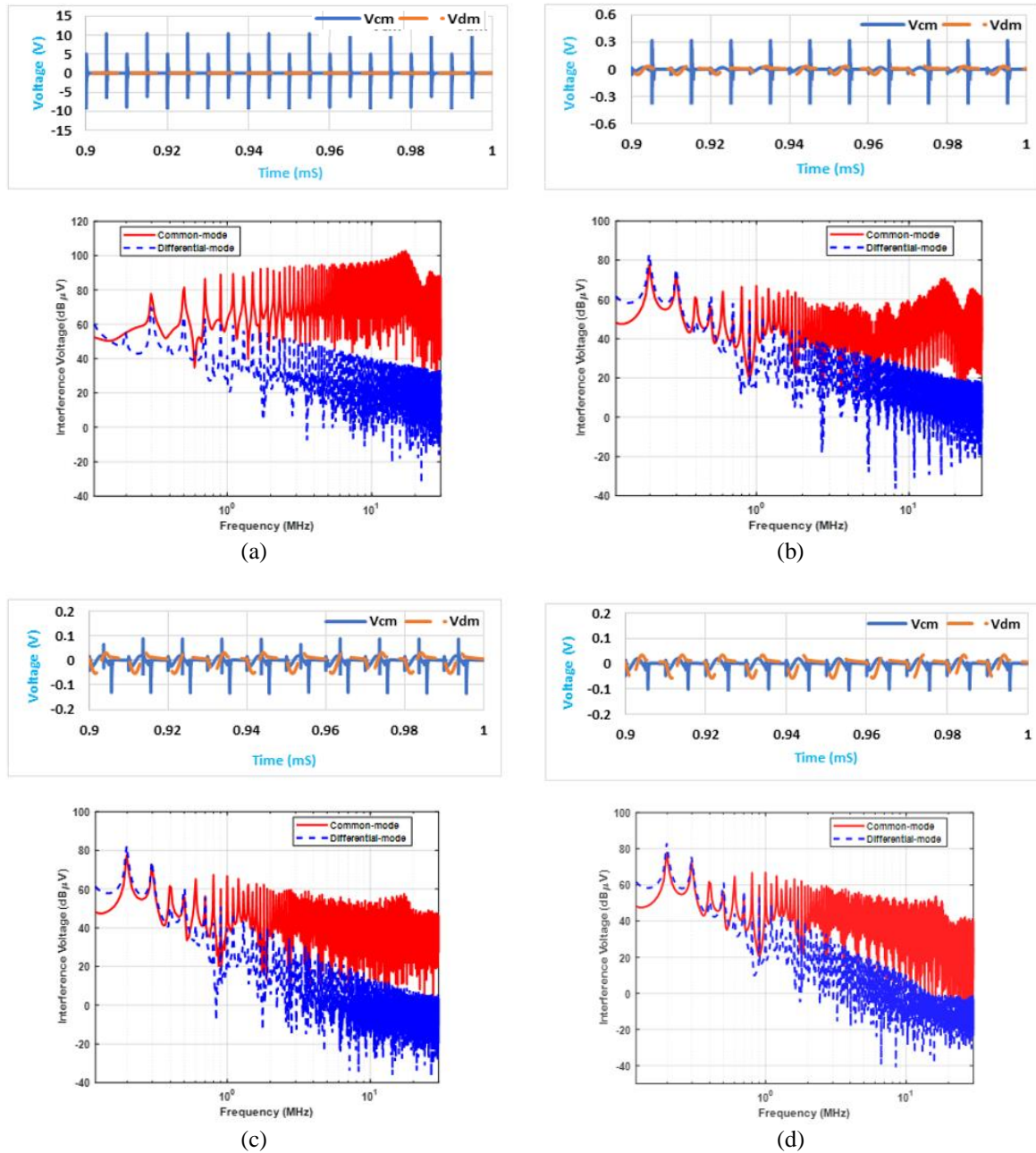

(a)   (b)

(c)   (d)

Figure 13. Frequency spectrum of differential and common mode disturbances localized on the RSIL for (a) DPWM method, (b) ZCS method, (c) ZCS-PI method, and (d) ZCS-FLC method

The complete study of the results in Figure 13 reveals, first and foremost, the efficiency of the ZCS technique when compared to the conventional one. A ZCS topology allows you to take advantage of the transistor's reverse conduction and increase the structure's linearity (the output voltage is less sensitive to the output current) [24]. Adopting a quasi-resonant form allows for soft switching of the switches, which helps reduce current gradients and limit capacitive coupling excitation.

Compared to the hard switching technique, the soft switching technique gives a substantially lower slope of the switching current I_{mos}, as seen in Figure 14. As a result, the resonant circuit's effect on EMI stresses is revealed. As can be seen, the value of the common mode voltage has been decreased by around 30 dBμV.
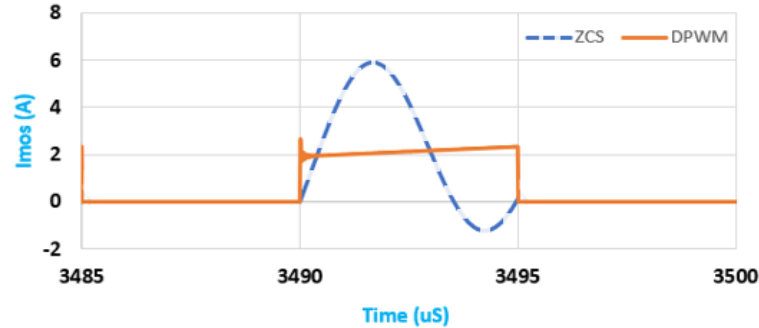

Figure 14. i_{mos} current slope for the DPWM and ZCS methods

After that, the ZCS approaches are compared with the open-loop, closed-loop PI controllers, and fuzzy controllers. By adjusting the pulse width modulation of the gate signal switching device, the fuzzy controller may efficiently reduce the amount of conducted interference generated in a buck converter. Utilizing the fuzzy controller reduces current and voltage strains in the soft-switching buck converter [25] and resonance phenomena caused by parasitic elements (capacitors and inductances). In the case of soft switching via a few control classes, Figure 15 displays the voltage waves of the master switch. When compared, it is clear that the highest peak of $\frac{dV_{mos}}{dt}$ at the main switch decreases when a fuzzy logic controller is used. As a result, the EMI will be significantly reduced.

This control is more efficient than a PI controller in electrical stress overshoot. Finally, this newly proposed solution achieves a considerable increase of roughly 35 dBμV in EMC by combining the benefits of the ZCS topology with a fuzzy logic control. The result reveals that the interference in this converter is kept within the CISPR-11 standard's limitations.
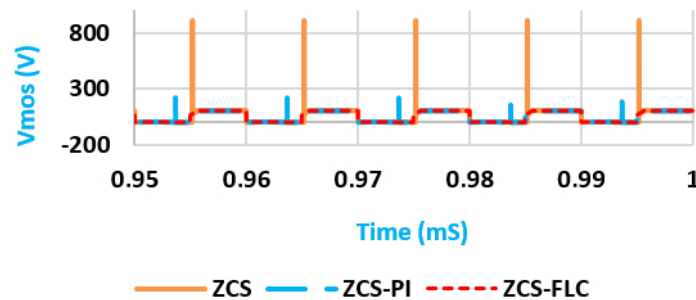

Figure 15. Waveform of device switch voltage under ZCS control conditions in open loop, closed loop by PI controller, and closed loop using fuzzy logic controller

5. CONCLUSION

Finally, static DC-DC converters like choppers have significant electromagnetic compatibility limits. As a result, they represent a severe risk to their control circuits and the surroundings (electromagnetic disturbances). An efficient strategy for reducing the negative impacts of common mode and differential mode conducted disturbances has been used in this study. It relies on resonant circuits to smooth the on-and-off switching. This technique includes the ZCS topology employed in the buck conversion system. It provides a significant reduction in the difficulty of transistor reverse recovery, decreasing the rate of rising di/dt current and obtaining a substantial EMC advantage.

The benefits of several forms of closed loop control dedicated to this ZCS structure, especially fuzzy logic and proportional-integral action control, will be discussed more below. The fuzzy logic controller delivers an exact output voltage without overshoot and seems to minimize voltage stress significantly. Based on spectrum analysis of conducted EMI, a comparative evaluation of this novel technique's effectiveness revealed that the tested device's conducted emissions were reduced considerably, and therefore EMC compliance was attained.

REFERENCES

[1]   M. Pahlavandust and M. R. Yazdani, "Single-switch boost DC-DC converter with zero-current-switching, high power density and low electromagnetic interference," *AEU-International Journal of Electronics and Communications*, vol. 121, Jul. 2020, doi: 10.1016/j.aeue.2020.153229.

[2]   Z. Li and D. Pommerenke, "EMI specifics of synchronous DC-DC buck converters," in *2005 International Symposium on Electromagnetic Compatibility, 2005. EMC 2005.*, 2005, vol. 3, pp. 711–714, doi: 10.1109/ISEMC.2005.1513616.

[3]   J. F. da Rocha, M. B. dos Santos, and J. M. D. Costa, "Voltage spikes in integrated CMOS Buck DC-DC converters: analysis for resonant and hard switching topologies," *Procedia Technology*, vol. 17, pp. 327–334, 2014, doi: 10.1016/j.protcy.2014.10.243.

[4]   P.-C. Chen, W.-C. Lin, M.-C. Tsai, G.-C. Hsieh, and H.-I. Hsieh, "Analysis, simulation and design of soft-switching mechanisms in DC to DC step-down converter," in *2019 IEEE 4th International Future Energy Electronics Conference (IFEEC)*, Nov. 2019, pp. 1–5, doi: 10.1109/IFEEC47410.2019.9015023.

[5]   V. Wuti, A. Luangpol, K. Tattiwong, S. Trakuldit, A. Taylim, and C. Bunlaksananusorn, "Analysis and design of a zero-voltage-switched (ZVS) quasi-resonant buck converter operating in full-wave mode," in *2020 6th International Conference on Engineering, Applied Sciences and Technology (ICEAST)*, Jul. 2020, pp. 1–4, doi: 10.1109/ICEAST50382.2020.9165351.

[6]   A. Ali, J. Chuanwen, M. Khan, S. Habib, and Y. Ali, "Performance evaluation of ZVS/ZCS high efficiency AC/DC converter for high power applications," *Bulletin of the Polish Academy of Sciences. Technical Sciences*, vol. 68, no. 4, 2020.

[7]   Y.-C. Chuang, "High-efficiency ZCS buck converter for rechargeable batteries," *IEEE Transactions on Industrial Electronics*, vol. 57, no. 7, pp. 2463–2472, Jul. 2010, doi: 10.1109/TIE.2009.2035459.

[8]   N. Shinde, S. Sankad, and S. L. Patil, "Design and study voltage characteristics of buck converter by Matlab Simulink," in *2018 2nd International Conference on Trends in Electronics and Informatics (ICOEI)*, May 2018, pp. 680–683, doi: 10.1109/ICOEI.2018.8553695.

[9]   K. Mittal, A. Jain, K. S. Vaisla, O. Castillo, and J. Kacprzyk, "A comprehensive review on type 2 fuzzy logic applications: Past, present and future," *Engineering Applications of Artificial Intelligence*, vol. 95, Oct. 2020, doi: 10.1016/j.engappai.2020.103916.

[10]   K. Bendaoud *et al.*, "Fuzzy logic controller (FLC): Application to control DC-DC buck converter," in *2017 International Conference on Engineering and MIS (ICEMIS)*, May 2017, pp. 1–5, doi: 10.1109/ICEMIS.2017.8272980.

[11]   F. L. Luo and H. Ye, "Investigation of EMI, EMS and EMC in power DC/DC converters," in *The Fifth International Conference on Power Electronics and Drive Systems, 2003. PEDS 2003.*, 2003, pp. 572–577, doi: 10.1109/PEDS.2003.1282904.

[12]   K. V. G. Raghavendra *et al.*, "A comprehensive review of DC–DC converter topologies and modulation strategies with recent advances in solar photovoltaic systems," *Electronics*, vol. 9, no. 1, Dec. 2019, doi: 10.3390/electronics9010031.

[13]   M. Laour, R. Tahmi, and C. Vollaire, "Modeling and analysis of conducted and radiated emissions due to common mode current of a buck converter," *IEEE Transactions on Electromagnetic Compatibility*, vol. 59, no. 4, pp. 1260–1267, Aug. 2017, doi: 10.1109/TEMC.2017.2651984.

[14]   C. Rostamzadeh, "Synchronous rectified step-down converter susceptibility to conducted and radiated EMI," in *2008 IEEE International Symposium on Electromagnetic Compatibility*, Aug. 2008, pp. 1–5, doi: 10.1109/ISEMC.2008.4652080.

[15]   A. Farhadi and A. Jalilian, "Modeling and simulation of electromagnetic conducted emission due to power electronics converters," in *2006 International Conference on Power Electronic, Drives and Energy Systems*, Dec. 2006, pp. 1–6, doi: 10.1109/PEDES.2006.344331.

[16]   B. Nassireddine, B. Abdelber, C. Nawel, D. Abdelkader, and B. Soufyane, "Conducted EMI prediction in DC/DC converter using frequency domain approach," in *2018 International Conference on Electrical Sciences and Technologies in Maghreb (CISTEM)*, Oct. 2018, pp. 1–6, doi: 10.1109/CISTEM.2018.8613398.

[17]   M. Laour, R. Tahmi, and C. Vollaire, "Experimental evaluation and FDTD method for predicting electromagnetic fields in the near zone radiated by power converter systems," *Turkish Journal of Electrical Engineering and Computer Sciences*, vol. 25, pp. 1460–1471, 2017, doi: 10.3906/elk-1506-278.

[18]   J. Bacmaga and A. Baric, "Modeling of conducted EM emissions of synchronous buck converters for different voltage conversion ratios," *IEEE Transactions on Electromagnetic Compatibility*, vol. 63, no. 6, pp. 2124–2133, Dec. 2021, doi: 10.1109/TEMC.2021.3069546.

[19]   Z. M'barki, K. S. Rhazi, and Y. Mejdoub, "A proposal of structure and control overcoming conducted electromagnetic interference in a buck converter," *International Journal of Power Electronics and Drive Systems (IJPEDS)*, vol. 13, no. 1, pp. 380–389, Mar. 2022, doi: 10.11591/ijpeds.v13.i1.pp380-389.

[20]   M. R. Yazdani and M. Pahalvandust, "A single-switch ZCS boost converter with low conducted EMI," in *2019 International Aegean Conference on Electrical Machines and Power Electronics (ACEMP) and 2019 International Conference on Optimization of Electrical and Electronic Equipment (OPTIM)*, Aug. 2019, pp. 336–340, doi: 10.1109/ACEMP-OPTIM44294.2019.9007224.

[21]   K. Swathy, S. Jantre, Y. Jadhav, S. M. Labde, and P. Kadam, "Design and hardware implementation of closed loop buck converter using fuzzy logic controller," in *2018 Second International Conference on Electronics, Communication and Aerospace Technology (ICECA)*, Mar. 2018, pp. 175–180, doi: 10.1109/ICECA.2018.8474570.

[22]   N. I. Kani, B. V. Manikandan, and P. Perciyal, "A novel soft switching based fuzzy logic control for single phase inverter," *Applied Mechanics and Materials*, vol. 573, pp. 143–149, Jun. 2014, doi: 10.4028/www.scientific.net/AMM.573.143.

[23]   S. Maity *et al.*, "Performance analysis of fuzzy logic-controlled DC-DC converters," in *2019 International Conference on Communication and Signal Processing (ICCSP)*, Apr. 2019, pp. 165–171, doi: 10.1109/ICCSP.2019.8698113.

[24]   Y. Yinghua, G. Honglin, W. Xinhua, and T. Jinfei, "Study on soft switching technology to reduce electromagnetic interference of PWM inverter," *Energy Procedia*, vol. 17, pp. 384–390, 2012, doi: 10.1016/j.egypro.2012.02.110.

[25]   C. Suganya, N. Purushothaman, E. Lathamercy, and C. Balaji, "Reduction of conducted electromagnetic interference in constant current/constant voltage battery charger using fuzzy logic controller," *International Journal of Applied Engineering Research*, vol. 10, no. 20, pp. 18922–18927, 2015.

BIOGRAPHIES OF AUTHORS

Zakaria M'barki was born in Morocco in 1990. He is a Ph.D. student at the Laboratory of Networks, Computing Science, Telecommunication, and Multimedia (RITM), ESTC Casablanca, Hassan 2 University in Morocco. In 2014, he graduated with honors from Morocco's National School of Electricity and Mechanics with a degree in Electrical and Telecommunication Engineering. His research activities include the development of a control structure capable of optimizing electromagnetic emissions in power electronics converters. He also has research interests in renewable energy sources, FACTS, power systems, and control system applications. He can be contacted at email: mbarki.ensem@gmail.com.

Kaoutar Senhaji Rhazi qualified professor in Electrical Engineering; at the School of Technology in Casablanca. Morocco. A graduate engineer in electrical engineering from the Mohammadia School of Engineers (EMI) in Rabat. Morocco (in 1991). Had the research preparation certificate (CPR) in telecommunications Ph.D. in July 2006 (in electromagnetic compatibility). Passed academic qualification in the same field in 2014. Became higher education teacher in 2020. Current research interests are: 'power electronics' and 'electromagnetic compatibility'. She can be contacted at email: senhaji.ksr@gmail.com.

Youssef Mejdoub was born in Morocco, in 1980. He received his Ph.D. Thesis on Modeling of Multiconductor Transmission Lines, in 2014 from Cadi Ayyad University, Marrakech Morocco. Since 2016, he has been a Professor at the Superior school of technology (EST), University of Hassan II of Casablanca. He currently works at the Electrical Engineering Department, Superior school of technology. His current research interests are antennas, electromagnetic compatibility, and MTL lines. He can be contacted at email: ymejdoub@yahoo.fr or youssef.mejdoub@univh2c.ma.